Room-Temperature Spin Memory in Two-Dimensional Electron Gases

J. M. Kikkawa, I. P. Smorchkova, N. Samarth, D. D. Awschalom*

Time-resolved Kerr reflectivity of two-dimensional electron gases in II-VI semiconductors provides a direct measure of electron spin precession and relaxation over a temperature range from 4 to 300 kelvin. The introduction of *n*-type dopants increases the electronic spin lifetimes several orders of magnitude relative to insulating counterparts, a trend that is also observed in doped bulk semiconductors. Because the electronic spin polarization in these systems survives for nanoseconds, far longer than the electron-hole recombination lifetime, this technique reveals thousands of spin precession cycles of 15 gigahertz per tesla within an electron gas. Remarkably, these spin beats are only weakly temperature dependent and persist to room temperature.

Extending spin coherence times in semiconductors is currently of great interest to those seeking to utilize coherent dynamics within practical devices (*1*). Recent discoveries (*2*) that spin ensembles can be used collectively as single quantum elements have renewed optimism that coherent electronics will eventually be realized as a basis for computation. Semiconductors offer the advantage that spin orientation of carriers (electrons and holes) induces strong optical nonlinearities that may be used to establish and probe electronic coherences (*3*, *4*). Here we use time-resolved magneto-optical techniques (*5*, *6*) to initiate and monitor electronic spin precession in modulation-doped II-VI semiconductor quantum wells (QWs). Remarkably, we found that in the presence of a two-dimensional electron gas (2DEG), the sample sustained this dynamical spin polarization for nearly three orders of magnitude longer than did insulating samples at low temperatures. Moreover, the spin lifetime surpassed the recombination lifetime by one to two orders of magnitude, which suggests that the 2DEG acquires a net polarization either through energy relaxation of spin-polarized electrons or through angular-momentum transfer within the electronic system. Our studies further showed that these nanosecond spin lifetimes persist to room temperature. Measurements on bulk epilayers revealed similar effects, even for low doping levels, and showed that these phenomena are not restricted to quantum-confined electronic systems. These findings demonstrate that external contributions to electronic spin decoherence are substantially reduced in these solid-state systems.

J. M. Kikkawa and D. D. Awschalom, Department of Physics, University of California, Santa Barbara, CA 93106, USA.
I. P. Smorchkova and N. Samarth, Department of Physics, The Pennsylvania State University, University Park, PA 16802, USA.
*To whom correspondence should be addressed.

The samples studied were modulation-doped II-VI semiconductor QWs recently developed as hosts for making magnetic 2DEGs (*7*). To explore the role of ionized impurity scattering and interface scattering, we used three 2DEG samples (A, B, and C) with different mobilities and growth characteristics. Each contained a strained 10.5-nm $Zn_{1-x}Cd_xSe$ QW ($x \sim 0.20$) with Cl-doped ZnSe barriers, grown by molecular beam epitaxy on a semi-insulating (100) GaAs substrate. Sample A was a symmetrically doped QW with 11-nm ZnSe spacer layers separating the QW from the 25-nm *n*-type ZnSe doping layers (doping concentration $n \sim 5 \times 10^{17}$ cm^{-3}). A 0.8-μm ZnSe buffer layer separated the QW structure from the GaAs substrate. Sample B was similar but had 12-nm spacers, 20-nm doping layers ($n \sim 10^{17}$ cm^{-3}), and a 1.6-μm buffer layer. Sample C was not symmetrically doped, as the QW was grown directly atop a 2.5-μm buffer layer, followed by a 12-nm spacer and a 20-nm doping layer ($n \sim 10^{17}$ cm^{-3}). Finally, sample D was an undoped, insulating 12-nm ZnSe/$Zn_{1-x}Cd_xSe$ QW ($x \sim 0.23$), also grown on a (100) GaAs substrate. All 2DEG samples showed clear integer quantum Hall effects and Shubnikov–de Haas oscillations in transport measurements carried out at temperatures $T < 4.2$ K and in fields $B > 2$ T; low-field Hall measurements were used to determine the 2DEG sheet densities and mobilities (Table 1).

Optical measurements were performed in a magneto-optical cryostat in fields up to 8 T and at temperatures ranging from 4 to 300 K. Static photoluminescence (PL) measurements indicated similar PL linewidths and intensities for both 2DEG and insulating samples. Static optical absorption in the 2DEG samples, however, was significantly reduced relative to that in their insulating counterparts; there was a weak, non-excitonic absorption edge (~1%) several millielectron volts above the PL emission, with this Stokes shift arising from a Moss-Burstein type bleaching of low-energy electron states by the 2DEG (*8*, *9*). For dynamical measurements, we used the frequency doubled output of a mode-locked Ti:sapphire laser, which provided 100-fs pulses at a repetition rate of 76 MHz. A conventional delay line yielded time delays between the pump and the probe of up to 1 ns. We obtained longer times (up to 13 ns) by using the frequency-doubled output of a second synchronously mode-locked Ti:sapphire laser, whose pulse train could be delayed relative to the first by simultaneously adjusting the cavity length in both lasers. An electronic feedback circuit programmed and maintained the relative delay with a time resolution of ~3 ps, although additional means can be used to reduce the jitter to less than 300 fs (*10*). A significant advantage of this two-laser cavity scheme is that pump and probe energies can be chosen independently.

Previous work (*5*, *6*) has demonstrated that low-temperature electron spin dynamics in semiconductor quantum structures can be directly measured by time-resolved Faraday rotation in the presence of an in-plane applied magnetic field (the Voigt geometry). Faraday rotation measurements on II-VI heterostructures are typically done in transmission and require the removal of the opaque GaAs substrate. To avoid introducing undesirable strain and depletion into these 2DEG systems through such processing, we used a modification of this technique (known as Kerr rotation) in which the probe is reflected off the sample. In this scheme (Fig. 1), a normally incident circularly polarized pump pulse creates electrons and holes with an initial spin orientation perpendicular to the applied magnetic field. The carrier spins subsequently precess about the magnetic field. The Kerr rotation θ_K of a linearly polarized time-delayed probe pulse sensitively detects the orientation of the carriers by rotating an amount proportional to their net spin along the direction of the probe. This rotation oscillates with the probe delay, thereby directly tracking the precession of the carrier spins. Spin-orbit coupling aligns the hole spins with the growth direction in QW samples, so that

Table 1. Sample characteristics measured at 4.2 K.

Sample	n (cm^{-2})	E_F (meV)	μ (cm^2 V^{-1} s^{-1})	g factor
A	5×10^{11}	8	2700	1.1
B	5×10^{11}	8	7900	1.1
C	2×10^{11}	3	6800	1.1
D	(insulating)	–	–	1.1

the hole spins do not precess in these systems (6) and the oscillatory signal can be unambiguously identified with the electron spin motion. In our experiment, the Kerr rotation of the reflected probe pulse was analyzed with a polarization beam-splitter and a conventional diode bridge (5, 6) capable of resolving rotations of 10^{-6} degrees. Studies were performed with an excitation energy E_{ex} at the heavy-hole absorption threshold in each sample, which corresponds to a spectral resonance in the measured Kerr rotation. While a photoelastic modulator switched the pump between right (σ^+) and left (σ^-) circular polarizations at 50 kHz, the probe intensity was chopped at ~2 kHz, and the resulting 48- and 52-kHz sidebands were recorded by standard lock-in techniques. We thereby obtained a measure of the probe's Kerr rotation induced by the orientation of the pump.

Figure 2A shows the low-temperature Kerr response of a 2DEG to a circularly polarized pump pulse in the presence of a 4-T in-plane magnetic field. Hundreds of oscillations in the Kerr rotation (resolved in the inset) represent the precession of the injected electron spins about the applied field. This precession arises from the quantum beating of energy-split spin states in the conduction band at a frequency ν, which is directly proportional to their spin splitting $\Delta E = h\nu$ (h, Planck's constant) along the direction of the applied field. The deduced g factors, $g = \Delta E/\mu_B H$ (μ_B, Bohr magneton; H, magnetic field), do not vary within the range of excitation powers and magnetic fields studied here and are only weakly temperature dependent below ~100 K. Thus, a single value can be used to characterize the low-temperature splittings in each sample, which we found to be nearly identical ($g \sim 1.1$) for both insulating and doped QW structures (Table 1).

Most striking is the contrast between the response of the 2DEG and that of the insulating sample. The envelope of the 2DEG spin polarization evolved on two time scales: a fast decay over the first 100 ps followed by a slower, secondary decay over several nanoseconds. The insulating QW (sample D) and other undoped samples exhibited a hundred-fold faster decay of the Kerr rotation and only one resolved oscillation, occurring at 4 T (Fig. 2B). A strength of this all-optical technique lies in its ability to directly resolve these decay profiles over both picosecond and nanosecond time intervals. Methods such as frequency-domain electron spin resonance typically infer such dynamical behavior from absorption linewidths. To understand the significance of the Kerr response, we note that because θ_K is sensitive to the net magnetization of the electrons, the decay of the oscillation envelope measures not only the number of precessing spins but also their directional alignment. The decay of the former is characterized by the homogeneous spin lifetime in a transverse field, T_2, whereas the latter is influenced by inhomogeneous effects that can introduce a progressive "dephasing" of precession angles within the spin population. Such inhomogeneous effects include local field variations or an energy-dependent g factor. We denote the net observed decay time as T_2^* and note that this may also include contributions from spin diffusion away from the probe area ~$(30\ \mu m)^2$. We do not believe that dephasing contributes significantly to T_2^*.

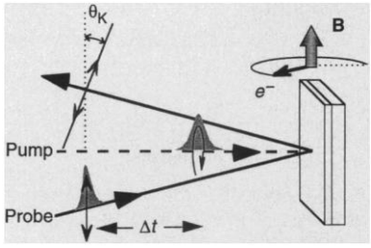

Fig. 1. A schematic of the experimental geometry. The probe's angle of incidence has been exaggerated for clarity. The time delay between the pump and the probe is indicated as Δt. A magnetic field is applied within the sample plane, inducing the precession of spin-polarized carriers. The probe polarization rotates an angle θ_K upon reflection, measuring the carrier spin normal to the sample surface.

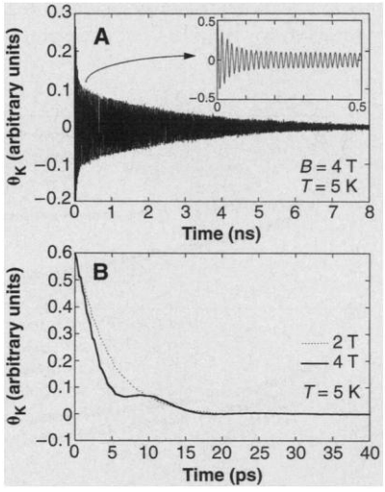

Fig. 2. (**A**) Time-resolved Kerr rotation of a 2DEG (sample C) at $T = 5$ K, $B = 4$ T, and an $E_{ex} = 2.70$-eV excitation, producing 5×10^{10} electrons cm^{-2} per pulse. (**Inset**) Oscillations over the initial decay period (axis labels remain unchanged). (**B**) The same as (A) for an insulating sample (sample D) at $T = 5$ K and $B = 2$ and 4 T, with 3×10^{11} electrons cm^{-2} per pulse and $E_{ex} = 2.63$ eV. Note the difference in time scales between (A) and (B).

To better understand the decay profiles (Fig. 2), we monitored carrier populations through time-resolved PL. Streak-camera measurements under nonresonant excitation were performed at the spectral peak of the QW emission. These measurements generally probe the hole lifetimes in 2DEG samples because electrons are always available for recombination (9); in insulating samples, the recombination lifetime reflects both carrier lifetimes. The hole lifetimes in the 2DEG samples were <50 ps and appear to correspond to the initial oscillation damping of 15 to 50 ps seen in these systems. These data suggest that electron-hole spin exchange (*11*), known to be important in intrinsic and *p*-doped systems (*12*, *13*), contributes to the initial electronic spin relaxation seen in the 2DEG samples. Similar measurements on the insulating system, sample D, revealed a PL lifetime of ~100 ps, which is then a lower limit for the hole lifetime and is much longer than their measured transverse spin lifetimes of 5 to 15 ps. In this insulating sample, we expect that the presence of excitons strengthens the electron-hole spin scattering through spin exchange, thus completely relaxing the electronic spins well within their lifetime. In contrast, the 2DEG samples had a shorter hole lifetime and a weaker electron-hole exchange, so that spin relaxation was incomplete and a remanent spin polarization precessed long after the holes had recombined. Because energy relaxation generally occurs well within the measured T_2^* times, we suspect that the electronic spin polarization, excited above the Fermi energy E_F, eventually relaxes into the 2DEG (*12*), where it precesses with dramatically reduced damping.

The measured oscillation amplitude can be reduced by the dephasing of spins as they precess, an inhomogeneous effect that masks the true transverse spin relaxation. Because the dephasing rate increases from zero as a magnetic field is applied, we looked for its contribution through the field dependence of θ_K, which would show an increased damping with increasing field. Figure 3A shows the low-temperature envelope of θ_K for sample C, plotted on a logarithmic scale for various fields. The slope of the decay is inverse to the spin lifetimes, which increased somewhat with applied field. This dependence suggests that dephasing is insignificant over this range of times and fields. We further expect this to be true for the insulating sample, where the spin lifetimes are only tens of picoseconds and dephasing contributions are expected to be similar.

A surprising aspect of the field dependence in all three 2DEG samples is that the application of a magnetic field up to 2 T

resulted in an increased total spin polarization remaining after the holes recombined. This behavior is detailed in Fig. 3B for sample C, where one can see that the amplitude of the oscillations at 2 T clearly surpasses the zero-field response. Beyond 2 T, there is no further increase in this amplitude, and the field-independence of the response at zero delay rules out artifacts due to changes in the Kerr sensitivity of the measurement with magnetic field. Although we do not fully understand the origins of the observed increase, we can gain insight through reflectivity measurements of the linearly polarized probe. These studies measure the transient carrier population at the laser energy, which is tuned just above E_F. This population decayed more rapidly as the applied field increased from 0.5 to 2 T (Fig. 3A, inset), beyond which it plateaued. Thus, there appears to be an inverse relation between the initial loss of electronic spin polarization and the relaxation of the nonequilibrium carrier population over this field range. One possible explanation is that the reflectivity changes arise from a decreased hole carrier lifetime. Although our streak camera PL measurements (resolution ~20 ps) do not resolve such a change, a shorter hole lifetime would reduce electron-hole spin scattering. Another possibility is that the transient reflectivity is convolved with carrier energy relaxation and that electron spin relaxation is more rapid during this process (*14*).

Among the three samples studied, there were significant sample-to-sample variations in the spin lifetimes measured at zero field. Although they all exhibited similar behavior up to 0.1 ns, the observed spin lifetime at later times was 2.3 ns for sample C, significantly longer than those found in samples A and B (0.53 and 0.40 ns, respectively) (Fig. 4A). In contrast to spin scattering data from standard models in which the momentum scattering plays a central role (*15, 16*), these data indicate little dependence on the sample mobility. Samples A and B have similar carrier densities (5×10^{11} cm^{-2}) but different mobilities (2700 and 7900 cm^2/Vs, respectively), and the spin relaxation is approximately the same. We are cautious about drawing any general conclusions here because the mobilities are characterized within a linear-response regime, whereas our optical measurements produced a highly nonequilibrium electron density whose momentum scattering rate could be substantially different. Nonetheless, we find no influence of excitation density on the decay rate in any of the samples (Fig. 4B, sample A), although increased electron densities will increase their momentum relaxation. Comparing samples B and C with essentially the same mobility, we note that decreasing the background carrier density 60% increases the spin lifetime nearly fivefold. Modest doping of these structures increased the spin lifetime well beyond that seen in insulating samples, but further doping might degrade their spin lifetimes. Although this behavior is consistent with models of spin relaxation in which energetic electrons have increased spin-scattering rates (*16*), these models also predict a stronger temperature dependence than we observe.

Figure 5A shows the envelope of the 2-T Kerr rotation for sample C at temperatures between 5.7 and 270 K. Although the extent of the initial depolarization seems to increase with temperature, the transverse lifetime for later times was only weakly temperature dependent, decreasing from 3.9 to 1.3 ns as the temperature was raised from 5.7 to 270 K. Thus, we resolved spin precession at room temperature (Fig. 5B). Furthermore, as the temperature was raised above 200 K, the resonance energy began to sharply decrease, and another energy resonance in the Kerr rotation appeared with nearly the same g factor but at an energy just above the room-temperature ZnSe band gap. Figure 5C shows the Kerr rotation at this energy, for which T_2* is 0.76 ns at room temperature and $B = 1$ T. We interpret this secondary resonance as arising from the equilibrium transfer of electrons from the 2DEG (producing a decrease in the Kerr resonance energy) into the ZnSe barriers at elevated temperatures. A depletion of the 2DEG complicates any detailed analysis of T_2* within the QW. In particular, one might expect that the inherent temperature dependence of T_2* in the QW may be even weaker than observed if one accounts for the depletion of the 2DEG.

Systematic studies on doped ZnSe epi-

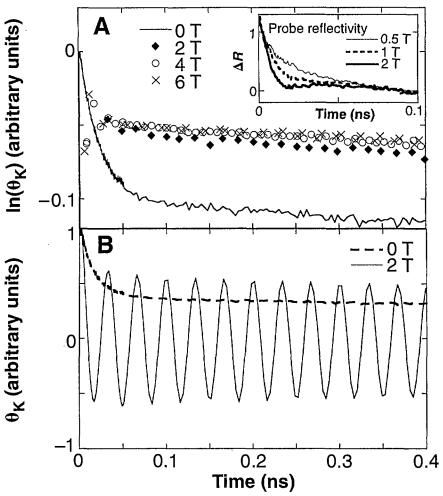

Fig. 3. (**A**) Kerr rotation at zero field (solid line) and the envelope of the oscillations seen at $B = 2$, 4, and 6 T. Data are plotted on a logarithmic scale. (**Inset**) Reflectivity (in arbitrary units) of a linearly polarized probe beam. (**B**) A comparison of the Kerr response at $B = 0$ and 2 T. All data is taken at 5 K on sample C with 5×10^{11} electrons cm^{-2} per pulse.

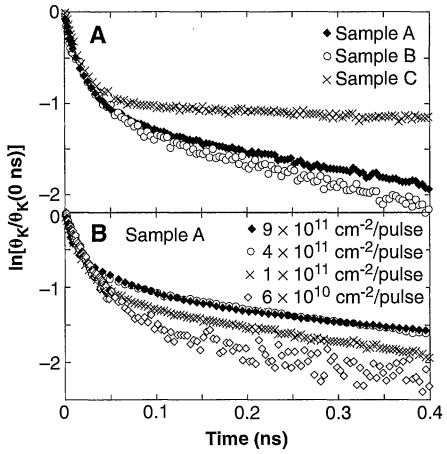

Fig. 4. (**A**) Natural logarithm of the zero-field Kerr rotation at $T = 5$ K for three different 2DEG samples taken with 10^{11} electrons cm^{-2} per pulse. (**B**) Dependence of the zero-field Kerr rotation on the density of electrons at $E_{ex} = 2.70$ eV. Data were taken on sample A at $T = 5$ K. Kerr rotations are normalized at zero delay.

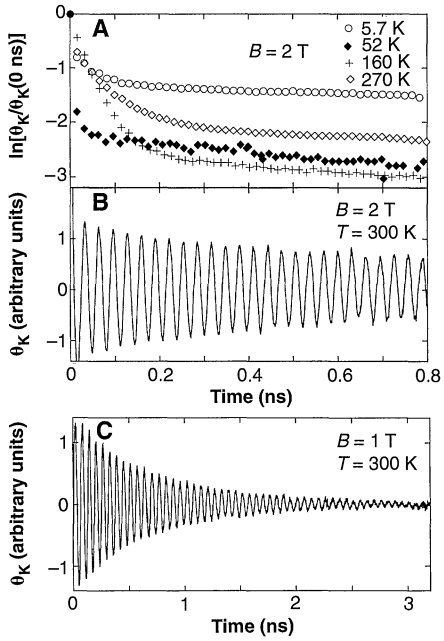

Fig. 5. (**A**) Envelopes of the measured Kerr rotation at $B = 2$ T in sample C taken with 10^{11} electrons cm^{-2} per pulse. The resonant excitation energy decreases from 2.70 to 2.61 eV as the temperature varies from 5.7 to 270 K. Amplitude changes have been normalized at zero delay. (**B**) Room-temperature Kerr rotation at 2 T in sample C at $E_{ex} = 2.60$ eV and 10^{11} electrons cm^{-2} per pulse. (**C**) Room-temperature Kerr rotation at 1 T in sample C with 5×10^{11} electrons cm^{-2} per pulse. The excitation is at $E_{ex} = 2.72$ eV, 20 meV above the ZnSe band-gap energy.

layers showed spin lifetimes of 1.6 ns at 275 K and equilibrium electron concentrations as low as 5×10^{16} cm^{-3} (*17*), suggesting that the room-temperature spin precession that we observed is a general feature of *n*-doped semiconductors. In fact, these bulk samples exhibited an even weaker temperature dependence than seen in the QW structures, with the spin lifetime decreasing only 20% from 5 to 300 K. Interestingly, for undoped samples, elevation of the temperature increased T_2* more than 10-fold above its low-temperature value, perhaps because of the thermal excitation of carriers or the thermal unbinding of excitons. For example, the precession lifetime at 2 T in the insulating QW (sample D) increased dramatically for temperatures above 80 K, rising from ~10 ps at 5 K to ~0.2 ns at 240 K. Similar behavior was seen in undoped ZnSe, where T_2* was only a few picoseconds at 4 K but increased to 0.3 ns at 270 K.

We have demonstrated an optically active solid-state system in which electron spin polarization persisted for nanoseconds at room temperature. It appears that a primary function of the electron gas is to sweep holes out of the system, terminating the highly efficient electron-hole spin scattering. The Kerr effect is an essential tool for viewing this process, as the phenomenon occurs for electrons above E_F and is invisible to measures of spin relaxation such as the Hanle effect or time-resolved PL, which probe electrons near zero momentum. This technique allows us to witness spin lifetimes that far exceed the carrier recombination time and draws an interesting contrast to systems in which carrier recombination depletes the spin polarization an order of magnitude faster than spin relaxation processes (*13*, *18*). We anticipate further insights into these spin relaxation processes with the extension of the time-resolved Kerr rotation technique to doped III-V semiconductors where both the elastic and inelastic scattering times are typically two orders of magnitude greater than in the samples studied here.

Although the observed precession reveals a memory of the initial spin orientation within the electronic system, its relation to individual spin coherence is not clear. Although electron-electron spin interactions of the form $\mathbf{s}_i \cdot \mathbf{s}_j$ can destroy the coherence of individual spins with their initial orientation established by the optical field, they would have no impact on the measured Kerr signal because they do not alter the equations of motion for total electronic spin. These "hidden" decoherences rely on the absence of any spatial dependence to the spin interaction that would then couple to the orbital degrees of freedom, permitting spin relaxation. Because we cannot rule out such hidden processes, only a direct interference experiment (*3*, *4*) can reveal the duration of quantum coherence within the spin precession. What we demonstrate here is that the contribution to spin decoherence from all other sources is quite small, even at room temperature. If these systems do prove to be quantum coherent for nanoseconds at room temperature, the development of ultrafast optical techniques to coherently manipulate the spin system would offer new technological opportunities.

REFERENCES AND NOTES

1. D. P. DiVincenzo, *Science* **270**, 255 (1995).
2. N. A. Gershenfeld and I. L. Chuang, *ibid.* **275**, 350 (1997).
3. S. Bar-Ad, I. Bar-Joseph, Y. Levinson, H. Shtrikman, *Phys. Rev. Lett.* **72**, 776 (1994).
4. A. P. Heberle, J. J. Baumberg, K. Kohler, *ibid.* **75**, 2598 (1995).
5. S. A. Crooker, J. J. Baumberg, F. Flack, N. Samarth, D. D. Awschalom, *ibid.* **77**, 2814 (1996).
6. ———, *Phys. Rev. B*, in press.
7. I. P. Smorchkova, N. Samarth, J. M. Kikkawa, D. D. Awschalom, *Phys. Rev. Lett.* **78**, 3571 (1997).
8. E. Burstein, *Phys. Rev.* **93**, 623 (1954).
9. G. Livescu *et al.*, *IEEE J. Quantum Electron.* **24**, 1677 (1988).
10. S. A. Crooker, F. D. Betz, J. Levy, D. D. Awschalom, *Rev. Sci. Instrum.* **67**, 2068 (1996).
11. G. L. Bir, A. G. Aronov, G. E. Pikus, *Zh. Eksp. Teor. Fiz.* **69**, 1382 (1975) [*Sov. Phys. JETP* **42**, 705 (1976)].
12. T. C. Damen, L. Vina, J. E. Cunningham, J. Shah, L. J. Sham, *Phys. Rev. Lett.* **67**, 3432 (1991).
13. J. Wagner, H. Schneider, D. Richards, A. Fischer, K. Ploog, *Phys. Rev. B* **47**, 4786 (1993).
14. F. Meier and B. P. Zakharchenya, Eds., *Optical Orientation* (North-Holland, Amsterdam, Netherlands, 1984).
15. R. J. Elliot, *Phys. Rev.* **96**, 266 (1954); F. Beuneu and P. Monod, *Phys. Rev. B* **18**, 2422 (1978).
16. M. I. D'yakanov and V. I. Perel', *Zh. Eskp. Teor. Fiz.* **60**, 1954 (1971) [*Sov. Phys. JETP* **33**, 1053 (1971)].
17. J. M. Kikkawa, I. P. Smorchkova, N. Samarth, D. D. Awschalom, unpublished results.
18. Ph. Roussignol *et al.*, *Phys. Rev. B* **46**, 7292 (1992); I. V. Kukushkin and V. B. Timofeev, *Adv. Phys.* **45**, 147 (1996).

19. Supported by grants from the Office of Naval Research (ONR N00014-97-1-0575 and N00014-97-1-0577) and the NSF Science and Technology Center for Quantized Electronic Structures (DMR 91-20007).

28 May 1997; accepted 10 July 1997

Synthesis of Gallium Nitride Nanorods Through a Carbon Nanotube–Confined Reaction

Weiqiang Han, Shoushan Fan,* Qunqing Li, Yongdan Hu

Gallium nitride nanorods were prepared through a carbon nanotube–confined reaction. Ga_2O vapor was reacted with NH_3 gas in the presence of carbon nanotubes to form wurtzite gallium nitride nanorods. The nanorods have a diameter of 4 to 50 nanometers and a length of up to 25 micrometers. It is proposed that the carbon nanotube acts as a template to confine the reaction, which results in the gallium nitride nanorods having a diameter similar to that of the original nanotubes. The results suggest that it might be possible to synthesize other nitride nanorods through similar carbon nanotube–confined reactions.

The fabrication of nanometer-sized materials has gained considerable attention because of their potential uses in both mesoscopic research and the development of nanodevices. Here, we demonstrate the synthesis of crystalline GaN nanorods (nanowires) based on the recently discovered carbon nanotubes (*1*). GaN has promising applications for blue and ultraviolet optoelectronic devices and has attracted much attention recently after the successful fabrication of high-efficiency blue light–emitting diodes (*2*). Several approaches have been developed for synthesizing nanocrystalline GaN powder (*3*). To our knowledge, the synthesis of GaN nanorods (or nanowires) has not been reported to date.

Department of Physics and Center of Atomic and Molecular Sciences, Tsinghua University, Beijing 100084, China.

*To whom correspondence should be addressed. E-mail: fss-dmp@mail.tsinghua.edu.cn

Recently, Dai *et al.* (*4*) reported an approach to the synthesis of nanoscale structures based on carbon nanotubes, in which the nanotubes were converted into carbide (MC) nanorods by reaction with a volatile oxide species. The reaction used was expressed as

$$\mathrm{MO(g)} + \mathrm{C(nanotubes)} \rightarrow \mathrm{MC(nanorods)} + \mathrm{CO} \qquad (1)$$

where MO is a volatile metal or nonmetal oxide with a relatively high vapor pressure at the desired reaction temperature. Further studies on the formation of the carbide nanorods have suggested that the very stable carbon nanotube might act as a template, spatially confining the reaction to the nanotube, which results in the formation of nanorods (*5*, *6*). We speculated that the method used to prepare carbide nanorods could be exploited to prepare